Nature and cause of compositional variation among the alkalic cap lavas of Mauna Kea Volcano, Hawaii

H.B. West[1], M.O. Garcia[1], F.A. Frey[2], and A. Kennedy[2]

[1] Hawaii Institute of Geophysics, University of Hawaii, Honolulu, HI 96822, USA
[2] Department of Earth, Atmospheric, and Planetary Sciences, Massachusetts Institute of Technology, Cambridge, MA 02139, USA

Abstract. Most Hawaiian basaltic shield volcanoes are capped by moderately to strongly evolved alkalic lavas (MgO < 4.5 wt.%). On Mauna Kea Volcano the cap is dominantly composed of hawaiite with minor mugearite. Although these lavas contain dunite and gabbroic xenoliths, they are nearly aphyric with rare olivine and plagioclase phenocrysts and xenocrysts. The hawaiites are nearly homogeneous in radiogenic isotope ratios (Sr, Nd, Pb) and they define coherent major and trace element abundance trends. These compositional trends are consistent with segregation of a plagioclase-rich cumulate containing significant clinopyroxene and Fe-Ti oxides plus minor olivine. Elements which are usually highly incompatible, e.g., Rb, Ba, Nb, are only moderately incompatible within the hawaiite suite because these elements are incorporated into feldspar (Rb, Ba) and oxides (Nb). However, in the most evolved lavas abundances of the most incompatible elements (P, La, Ce, Th) exceed (by $\sim$ 5–10%) the maximum enrichments expected from models based on major elements. Apparently, the crystal fractionation process was more complex than simple, closed system fractionation. The large amounts of clinopyroxene in the fractionating assemblage and the presence of dense dunite xenoliths with CO_2 inclusions formed at minimum pressures of 2 kb are consistent with fractionation occurring at moderate depths. Crystal segregation along conduit or magma chamber walls is a possible mechanism for explaining compositional variations within these alkalic cap lavas.

Introduction

Hawaiian volcanoes follow a well established evolutionary path (Macdonald et al. 1983). The bulk of each volcano (95–99%) is presumed to be tholeiitic basalt although less than 20% of the total thickness is exposed at any Hawaiian volcano. On most Hawaiian volcanoes (e.g., Mauna Kea, Hualalai, Kohala, Haleakala, West Maui, Waianae) a relatively thin sequence (10–300 m thick) of evolved alkalic lavas "cap" the tholeiitic shield-forming lavas. These lavas are predominantly hawaiites and mugearites with minor or no benmoreites and trachytes. Relative to the shield building stage, the alkalic cap stage is a period of substantially

reduced volcanic activity, apparently reflecting a decreasing supply of magma (Feigenson and Spera 1981; Wise 1982; Clague 1987; Spengler and Garcia 1988); hence, this stage represents a marked change in the development of Hawaiian volcanoes.

Mauna Kea is an excellent volcano for the study of alkalic cap lavas because the stratigraphy has been well-documented (Porter 1979; Wolfe 1987) and the lavas are generally very fresh due to: (1) their young age (< 0.3 Ma; Porter 1979), (2) exposure at high elevation (up to 4.2 km), and (3) the low rainfall (above 2 km elevation). This study focuses on the south rift zone of the Mauna Kea Volcano because it has the widest temporal range of lavas from the alkalic cap stage. Previous studies (Macdonald and Katsura 1964; Macdonald 1968) have shown that the alkalic cap lavas at Mauna Kea are dominantly hawaiites with rare mugearite.

In this paper, major and trace element data for 39 lavas and radiogenic isotopic data for 8 lavas are utilized to evaluate the spatial and temporal compositional variations of alkalic cap lavas and to model the processes causing compositional variations within the alkalic cap suite. There is no systematic relationship between temporal or spatial variation and the composition of alkalic-cap lavas. Nevertheless, compositional variations of these lavas define coherent trends and there is very little variation in Pb, Sr and Nd isotope ratios. These coherent compositional trends can largely be explained by fractionation of a plagioclase-rich assemblage containing significant amounts of clinopyroxene, Fe-Ti oxides and olivine. The major element compositional trends and presence of dunite and gabbroic xenoliths are consistent with fractionation at pressures of at least 2 kb.

Regional Geology of Mauna Kea

Mauna Kea is the highest of the five principal volcanoes on the island of Hawaii, rising to a height of 4205 m (Fig. 1). Most (87.5%) of the volcano is submarine and a minimum volume estimate is 2.5×10^4 km³ (Bargar and Jackson 1974). Shield-building volcanism appears to have been concentrated along two principal rift zones (east and west). A third minor rift zone trends south. Vents for alkalic cap lavas are not confined to the rift zones and are widely distributed on the volcano at elevations of 2 km or greater above sea level (Fig. 1).

Stratigraphically, the lavas of Mauna Kea have been separated into two units: a lower "shield-building" sequence, designated the
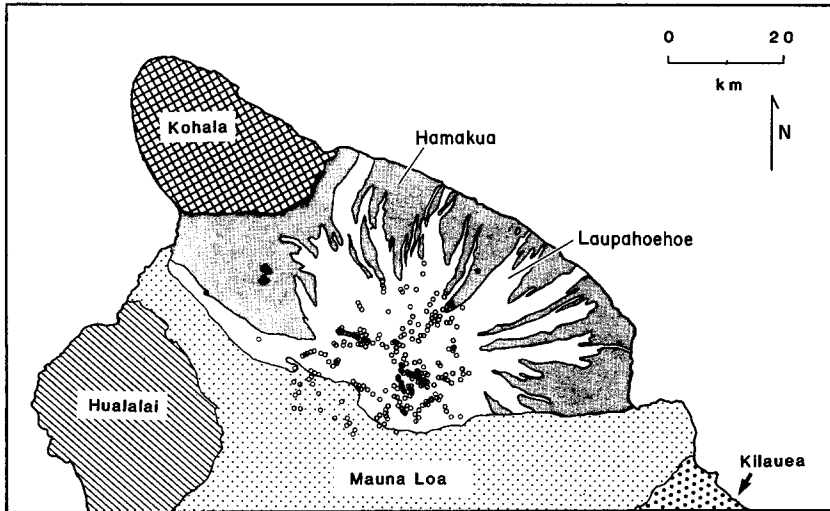
Fig. 1. Map of the northern half of the Island of Hawaii showing the distribution of lavas from the five volcanoes comprising the island. Mauna Kea is subdivided into the shield lavas of the Hamakua Group (*shaded area*) and the alkalic cap lavas of the Laupahoehoe Group (unshaded area). Vents for the Laupahoehoe lavas are shown by the open circles (after Stearns and Macdonald 1946 and Porter 1979)
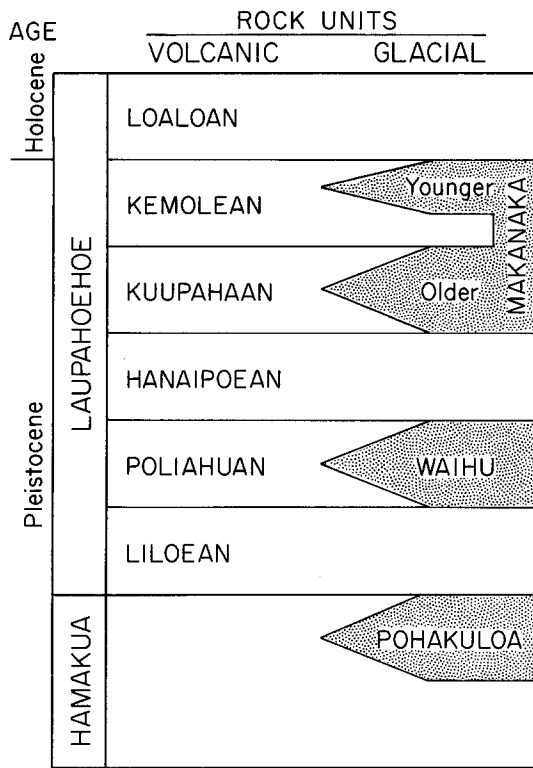

Fig. 2. Generalized stratigraphic sequence for volcanic and glacial rock units from Mauna Kea Volcano, Hawaii (after Porter 1979)

its that enabled Porter (1979) to divide the Laupahoehoe Group into six stages (Fig. 2). Wolfe (1987) recently completed a detailed mapping study of the Laupahoehoe lavas and he proposed only two units: Pleistocene (combining 5 of Porter's units) and Holocene (which is identical to Porter's Loaloan unit). Porter's (1979) stratigraphy is utilized here in an attempt to evaluate the temporal evolution of Laupahoehoe lavas. Because we found no systematic compositional changes with eruption age, our interpretations are not affectd by the alternative stratigraphic interpretations.

Laupahoehoe volcanism probably began ~65 ka (Wolfe, 1987) and the most recent eruption was about 4.4 ka ago (Porter 1979). Based on air photo interpretation, there were about 65 distinct eruptions during the upper and middle stages of the Laupahoehoe Group and about 6 eruptions during the uppermost stage. This yields an average of about 1 eruption per 1250 years for the upper and middle stages and about 1 eruption per 1500 years for the uppermost stages. The lower Laupahoehoe stage eruption rate could not be determined because many of its vents are covered by later lavas and glacial sediments. Recent estimates for Kohala are similar (but less frequent) than the Laupahoehoe estimates (1 eruption per 1900 years; Spengler and Garcia, 1988). The lower eruption rate for Kohala is consistent with a much larger proportion (~43%) of highly evolved lava, mugearite to trachyte (Spengler and Garcia, 1988). Eruption rates for alkalic-cap lavas from Mauna Kea are much lower than those for an active tholeiitic shield like Kilauea (1 eruption every 1 to 4 years; Klein, 1982; Dzurisin et al. 1984) and significantly lower than the eruption rate (1 eruption per 50 years; Moore et al. 1987) of alkalic basalts on Hualalai volcano which has not yet reached the alkalic cap stage. This trend of decreasing eruption rate with age must reflect movement of the volcano away from the mantle "hot-spot".

Sample Locations

Thirty-nine Laupahoehoe Group lavas were collected from the summit and south rift zone of Mauna Kea and were analyzed for major and trace elements (Table 1). These samples were collected only from cinder cones and flows which Porter (1979) placed within one of the six volcanic stages. All stages were sampled so that compositional evolution of the alkalic cap lavas could be evaluated. In addition, the collected lavas span a wide range in elevation (2255 m) and distance from the summit (0–14 km) and thus represent a wide spatial distribution. Vents from the various stages are not evenly distributed on the slopes of the volcano. Lavas from the youngest and oldest stages tend to be concentrated on the flanks of the volcano; lavas from the middle stages are most common near the summit.

Hamakua Group, and an upper alkalic cap stage, designated the Laupahoehoe Group (Stearns and Macdonald 1946; Porter 1979). The Hamakua Group lavas range in age from 80 to greater than 150 ka (Wise 1987) and in composition from tholeiite to alkalic basalt with some ankaramites and high TiO_2 hawaiites (Frey et al. 1987). Laupahoehoe lavas are well exposed on the upper slopes of the volcano and within some gulches on the east flank. The total thickness of Laupahoehoe Group lavas is unknown. Estimates of thickness vary from as little as 10 m on the lower flanks of the volcano (Stearns and Macdonald 1946) to as great as 550 m at the summit (assuming the lavas filled a caldera; Porter 1972). The upper portion of Mauna Kea has been glaciated and deposits from the glacial activity are interstratified with lavas from the Laupahoehoe Group. These glacial deposits are time-stratigraphic un-

Table 1. Major and trace elements contents of Laupahoehoe lavas, Mauna Kea Volcano, Hawaii. Stages are in order of increasing age; samples within a stage are in order of decreasing MgO

	Loaloan															
	Ml-5	Ml-18	Ml-4	Ml-19	Ml-6	Ml-17	Ml-14	Ml-15	Ml-3	Ml-2	Ml-20	Ml-7	Ml-11	Ml-8	Ml-13	Ml-12
SiO_2	51.22	50.77	50.64	50.78	50.77	50.84	50.67	50.75	50.67	50.58	51.90	52.03	52.38	52.56	52.58	52.83
TiO_2	2.59	2.63	2.60	2.60	2.56	2.58	2.60	2.59	2.56	2.58	2.32	2.19	2.18	2.23	2.21	2.05
Al_2O_3	17.31	17.22	17.08	17.19	17.12	17.16	17.13	17.10	17.12	16.88	17.12	17.18	17.18	17.57	17.29	17.28
Fe_2O_3	11.17	11.34	11.23	11.28	11.11	11.30	11.26	11.34	11.27	11.12	10.59	10.52	10.48	10.63	10.58	10.14
MnO	0.22	0.22	0.22	0.22	0.22	0.22	0.22	0.22	0.22	0.21	0.21	0.23	0.23	0.23	0.23	0.24
MgO	3.97	3.95	3.94	3.93	3.92	3.91	3.88	3.88	3.86	3.81	3.52	3.40	3.36	3.33	3.31	3.11
CaO	6.69	6.72	6.67	6.65	6.63	6.69	6.73	6.67	6.60	6.60	6.22	6.14	6.13	6.08	6.17	6.03
Na_2O	4.50	4.56	4.53	4.63	4.48	4.52	4.61	4.11	4.69	5.11	5.14	4.79	4.83	4.66	4.84	4.84
$Na_2O(NA)$		4.74							4.84	4.54	4.75					5.11
K_2O	1.96	1.92	1.94	1.95	1.96	1.95	1.95	1.95	1.95	1.95	2.13	2.14	2.16	2.15	2.17	2.16
P_2O_5	0.88	0.90	0.88	0.90	0.88	0.90	0.91	0.90	0.92	0.87	0.95	1.04	1.04	1.06	1.08	1.13
SUM	100.51	100.23	99.73	100.13	99.65	100.07	99.67	99.51	99.86	99.71	100.10	99.66	99.97	100.50	100.46	99.81
Fe_2O_3/FeO	0.43	0.77	0.38	0.66	1.09	–	0.86	0.52	0.97	0.45	0.79	–	0.41	11.1	1.30	–
H_2O^+	0.30	0.37	0.28	0.32	0.23	–	0.38	0.24	0.21	0.30	0.27	–	0.40	0.53	0.38	–
H_2O^-	0.16	0.14	0.11	0.10	0.08	–	0.19	0.09	0.10	0.15	0.14	–	0.20	0.26	0.13	–
CO_2	0.03	0.03	0.06	0.09	0.08	–	0.11	0.03	0.09	0.03	0.11	–	0.10	0.06	0.04	–
Rb	33.6	35.5	34.6	36.4	37.9	35.2	33.7	34.7	35.9	36.0	39.0	37.2	42.6	40.6	41.2	35.5
Sr	1281	1254	1280	1269	1273	1275	1262	1261	1260	1265	1222	1242	1244	1241	1244	1241
Ba	627	618	634	645	631	648	630	670	643	639	652	695	703	697	695	736
Sc		9.0				–			8.7	8.8	7.6	–				6.7
V	71	74	71	74	72	70	75	80	73	68	60	45	46	49	43	42
Cr		3.5							2.6	2.4	3.4					4.9
Ni	3	7	5	10	5	5	9	15	8	8	6	6	2	8	6	15
Zn	129	139	135	129	125	137	141	129	135	129	139	133	148	148	127	138
Ga	22.4	22.3	23.2	22.2	22.2	22.8	22.5	21.3	23.2	21.7	22.5	23.5	23.0	21.9	23.5	22.7
Y	45	44	44	44	44	44	44	44	44	43	44	48	48	48	48	49
Zr	487	466	489	474	481	481	479	474	507	495	503	550	536	537	534	561
Nb	62.2	62.6	63.2	62.4	61.0	63.8	63.8	61.8	62.3	63.6	66.7	68.4	69.8	67.5	67.9	71.3
Hf		10.3							9.9	10.1	10.8					12.3
Th		3.4							3.9	3.9	4.6					4.4
La		50.8							51.5	49.9	53.4					63.6
Ce		123							122	119	135					155
Ce(XRF)	115	117	120	111	117	121	119	116	117	114	128	133	136	128	132	143
Nd		66.6							65.0	62.0	70.6					82
Sm		14.0							13.9	13.5	14.4					16.6
Eu		4.44							4.60	4.56	4.56					5.07
Tb		1.97							1.70	1.75	1.69					2.16
Yb		3.41							3.22	3.31	3.26					3.88
Lu		0.45							0.46	0.44	0.48					0.57

Analytical

Mineral analyses were made with the University of Hawaii electron microprobe (Garcia et al. 1986). Major element contents and selected trace elements (Rb, Sr, Ba, V, Ni, Zn, Ga, Y, Zr, Nb and Ce) were determined in duplicate at the University of Massachusetts by X-ray fluorescence (XRF) (Rhodes, 1983). Ferrous iron was determined by titration, H_2O^+ by heating at 1100 ° with collection on anhydrone and CO_2 by HCl dissolution with collection on ascarite, all at the University of Manitoba. In addition, 19 samples were analyzed for Na, Sc, Cr, Hf, Th, and REE by instrumental neutron activation at MIT (Ila and Frey, 1984). Precision of the abundance data is indicated in Table 1; in addition, Na and Ce were analyzed by XRF and neutron activation (Table 1).

Nd, Sr, and Pb chemical and mass spectrometric techniques were adopted from Hart and Brooks (1977), Richard et al. (1976) and Grunenfelder et al. (1986). $^{87}Sr/^{86}Sr$ ratios are normalized to 0.70800 for E and A $SrCO_3$ and $^{143}Nd/^{144}Nd$ to 0.51264 for BCR-1 using $^{146}Nd/^{144}Nd = 0.72190$. Pb isotopic ratios are normalized to an SRM 981 value for ^{208}Pb /^{206}Pb of 2.1671 (Todt et al. 1984).

Results

Petrography and mineral compositions

The Lauaphoehoe Group samples studied are fresh and essentially aphyric. They contain rare (0–1.4 vol.%) plagioclase phenocrysts and less than 1.8 vol.% microphenocrysts (Table 2). Plagioclase is the dominant microphenocryst phase with subequal to lesser amounts of olivine and magnetite. Extremely rare (<0.1 vol.%) xenocrysts of olivine (resorbed and kinked) and plagioclase occur in some lavas. The lavas have a trachytic texture and range from sub-

386

Table 1 (continued)

	Kemolean						Kuupahaan					
	Mk-1	Mk-2	Mk-4	Mk-3	Mk-5	Mk-6	Me-2	Me-1	Me-6	Me-3	Me-4	Me-5
SiO_2	49.46	51.07	50.80	51.32	50.14	52.41	49.28	50.54	50.40	51.03	52.12	51.78
TiO_2	2.76	2.50	2.50	2.48	2.57	2.21	2.85	2.80	2.75	2.51	2.32	2.22
Al_2O_3	17.11	17.25	17.17	17.29	17.87	17.82	17.01	17.32	17.15	17.14	17.35	17.28
Fe_2O_3	11.48	10.72	10.70	10.68	11.15	10.03	11.44	11.40	11.42	10.83	10.39	10.20
MnO	0.21	0.21	0.21	0.21	0.22	0.22	0.21	0.22	0.22	0.22	0.22	0.22
MgO	4.14	3.77	3.74	3.73	3.70	3.28	4.20	4.16	4.12	3.74	3.48	3.27
CaO	6.97	6.66	6.66	6.62	6.91	6.11	7.04	7.00	6.98	6.59	6.36	6.38
Na_2O	4.84	4.83	5.03	4.80	4.80	4.93	4.61	4.32	4.56	4.60	4.82	5.16
Na_2O(NA)	4.60 ± 0.04	4				4.89	4.63		4.56			
K_2O	1.82	2.06	2.00	2.08	1.77	2.20	1.85	1.94	1.89	2.01	2.15	2.19
P_2O_5	0.85	0.96	0.95	0.95	1.10	1.06	0.84	0.91	0.86	0.91	0.97	1.11
SUM	100.14	100.03	99.76	100.16	100.24	100.27	99.33	100.61	100.35	99.58	100.18	99.81
Fe_2O_3/FeO	0.52	0.73	0.53	0.95	0.73	0.49	0.46	0.57	0.55	0.48	0.50	0.62
H_2O^+	0.20	0.36	0.32	0.37	0.53	0.70	0.12	0.40	0.40	0.15	0.30	0.23
H_2O^-	0.19	0.08	0.18	0.09	0.69	0.27	0.11	0.18	0.17	0.06	0.17	0.08
CO_2	0.10	0.02	0.06	0.06	0.09	0.05	0.09	0.04	0.07	0.03	0.07	0.04
Rb	31.9	38.6	37.3	38.7	25.6	40.7	34.3	35.7	34.3	38.3	35.5	41.3
Sr	1264	1260	1255	1230	1261	1190	1273	1246	1262	1248	1245	1230
Ba	623	652	631	657	656	800	576	600	587	615	651	656
Sc	9.8 ± 0.1					7.0	10.2		9.8			
V	88	67	61	67	60	58	97	87	85	71	64	46
Cr	8 ± 1					5.6	8.9		5.9			
Ni	7	8	10	9	10	4	4	9	12	5	3	7
Zn	149	129	130	130	139	169	116	131	133	128	141	132
Ga	22.7	21.3	21.9	21.9	21.1	23.0	21.4	23.2	22.2	23.5	22.7	22.4
Y	44	47	46	46	50	50	44	45	44	46	48	50
Zr	468	539	511	523	532	599	449	466	433	501	533	565
Nb	62.2	63.5	63.7	64.4	68.0	68.0	56.3	60.8	60.9	63.8	67.5	68.9
Hf	9.66.08					12.5	9.5		9.6			
Th	3.2 ± 0.2					4.9	3.1		3.5			
La	48.8 ± 0.8					60.9	45.8		48.1			
Ce	120 ± 1					143	113		117			
Ce(XRF)	11	117	119	119	136	142	117	120	118	124	132	141
Nd	66 ± 2					73.0	62.8		63.6			
Sm	14.53 ± 0.08					14.9	13.3		14.1			
Eu	4.56 ± 0.05					4.92	4.38		4.58			
Tb	1.87 ± 0.01					1.90	1.91		1.76			
Yb	3.26 ± 0.11					3.71	3.29		3.13			
Lu	0.44 ± 0.02					0.51	0.43		0.43			

pilotaxitic to hyalopilitic. The groundmass consists primarily of plagioclase, magnetite, olivine and clinopyroxene with rare apatite. The scarcity of phenocrysts and the fine-grained nature of the matrix justifies treating the whole-rock analyses as representative of liquid compositions.

Relative to the bulk rock (assuming $Fe^{+2} = 0.85$ molar Fe^T) groundmass olivine in Mi-5, the most mafic Laupahoehoe hawaiite (Table 3), yields a K_D [$(Fe/Mg)_{ol}/(Fe/Mg)_{WR}$] of 0.31 similar to the experimentally determined equilibrium value of ~ 0.3 (Roeder and Emslie, 1970). However, olivine microphenocrysts (<0.5 mm) in Mi-5 (Table 3) yield lower K_D's of ~ 0.20. These disequilibrium microphenocrysts are similar in composition (Fo 81) to strongly resorbed olivine xenocrysts, in a more evolved hawaiite (Mi-2, Tables 1 and 3). Microphenocrysts in Mi-2 yield near-equilibrium olivine/bulk-rock Fe^{+2}/Mg ratios of ~ 0.27.

Euhedral plagioclase phenocrysts in Laupahoehoe lavas range only from An_{57} to An_{59} (Table 3). These compositions yield a K_D [$(Ca/Na)_{plagioclase}/(Ca/Na)_{whole\ rock}$] of 1.75 which is higher than values obtained in experiments (1.1–1.6) by Mahood and Baker (1986) on similar rocks at temperatures greater than 1075 °C. The plagioclase xenocryst has a higher An content (72.5) than the euhedral grains and it is too calcic to be in equilibrium with the bulk rock. The opaque minerals are Ti-magnetites. Adjacent to rare dunite xenoliths, the magnetites are enriched in Cr and depleted in Ti (Table 3).

Whole rock geochemistry

Major elements. The compositions of Laupahoehoe Group lavas are typical of Hawaiian alkalic cap lavas and they

Table 1 (continued)

	Hanaipoean				Poliahuan		Liloean						
	Mh-2	Mh-3	Mh-1	Mh-4	Mp-2	Mp-1	Mi-5		Mi-2	Mi-3		Mi-4	Mi-1
SiO_2	50.96	52.06	51.94	51.61	50.14	51.31	49.70	49.26	50.47	52.44	52.46	52.30	52.73
TiO_2	2.36	2.29	2.23	2.15	2.74	2.41	2.95	2.96	2.65	2.02	2.04	2.04	2.00
Al_2O_3	17.14	17.44	17.34	17.10	17.07	17.37	17.06	16.89	17.25	17.58	17.62	17.70	17.43
Fe_2O_3	10.62	10.16	10.21	10.73	11.55	10.93	11.83	11.83	11.17	10.00	10.02	10.10	9.94
MnO	0.22	0.21	0.22	0.22	0.22	0.23	0.21	0.21	0.21	0.22	0.23	0.23	0.22
MgO	3.50	3.40	3.27	3.26	4.17	3.67	4.45	4.40	4.01	3.01	3.03	3.02	2.98
CaO	6.70	6.19	6.40	6.23	6.90	6.74	7.15	7.15	6.93	6.20	6.22	6.12	6.05
Na_2O	4.78	5.00	5.17	5.16	4.26	4.61	4.49	4.56	4.60	5.02	5.07	4.93	5.47
Na_2O(NA)	5.01	5.10	5.21	4.90	--	4.39	4.46±0.08	-	4.62±0.12	5.04±0.18		4.92	5.28
K_2O	2.14	2.18	2.19	2.22	1.88	2.15	1.84	1.82	1.95	2.26	2.26	2.23	2.32
P_2O_5	1.32	0.93	1.12	1.30	0.85	1.14	0.81	0.80	0.93	1.22	1.23	1.21	1.20
SUM	99.74	99.86	100.09	99.98	99.78	100.56	100.49	99.88	100.17	99.98	100.17	99.89	100.34
Fe_2O_3/FeO	0.70	0.43	0.66	0.67	0.40	0.77	0.44		0.74	2.34		0.48	0.66
H_2O^+	0.30	0.43	0.08	0.28	0.10	0.78	0.32		0.44	0.54		0.75	0.31
H_2O^-	0.22	0.10	0.09	0.10	0.05	0.72	0.08		0.18	0.19		0.29	0.09
CO_2	0.07	0.06	0.08	0.03	0.02	0.13	0.06		0.09	0.20		0.06	0.01
Rb	38.6	41.8	42.6	45.7	35.0	42.9	32.0		33.4	38.4		41.0	43.1
Sr	1223	1222	1220	1105	1283	1206	1260		1287	1178		1180	1169
Ba	660	677	649	677	605	630	562		613	687		693	690
Sc	7.7	7.5	7.0	7.7		8.0	10.6 ±0.1		9.3 ±0.2	6.6 ±0.2		6.7	6.6
V	56	53	48	40	87	55	109		84	35		36	38
Cr	3.0	5.9	6.4	3.6	--	3.3	11.0 ±0.4		7.4 ±0.8	5.3 ±0.1		6	8
Ni	7	7	4	5	12	10	4		8	11		7	7
Zn	136	130	129	140	123	136	133		129	142		145	153
Ga	21.8	21.5	21.8	23.0	22.2	23.1	22.9		21.5	22.4		23.3	22.8
Y	52	47	50	52	44	49	43		47	53		52	52
Zr	545	547	554	611	442	536	425		457	607		636	625
Nb	68.7	67.0	67.8	70.9	59.3	65.4	57.4		61.2	74.5		73.4	75.3
Hf	12.2	11.8	12.1	12.6		11.5	9.2 ±0.3		10.2 ±0.2	13.1 ±0.6		13.5	13.4
Th	5.9	4.4	4.4	4.9		4.3	3.2 ±0.2		3.4 ±0.1	4.8 ±0.1		4.9	5.0
La	62.0	54.8	59.3	66.7		57.4	44.5 ±0.7		50.9±0.1	65.6 ±1.3		66.7	67.5
Ce	155	131	142	156	117	140	108 ±3		124 ±3	158 ±7		157	155
Ce(XRF)	150	128	141	153		133	109		118	152		153	154
Nd	84	69	75	79		75	59±3		68±3	82±5		80	80
Sm	17.1	15.5	17.2	16.1		16.1	14.3		14.8 ±0.1	16.4 ±0.6		17.5	17.7
Eu	5.40	4.69	5.07	5.16		4.98	4.40±0.01		4.74±0.06	5.22±0.04		5.20	5.20
Tb	2.32	1.82	1.98	1.92		1.85	1.72±0.08		1.94±0.15	2.12±0.23		2.07	2.06
Yb	4.02	3.39	3.85	3.82		3.68	3-12±0.03		3.33±0.03	4.10±0.16		3.97	4.12
Lu	0.55	0.50	0.50	0.53		0.51	0.44±0.01		0.47±0.02	0.55±0.04		0.56	0.55

Notes: (1) Two Mi-5 major element analyses are for two independent sets of duplicates. (2) Two Mi-3 analyses are for two separate crushes of hand-specimen sample

are distinct from the underlying Hamakua shield lavas which are dominantly basaltic (Frey et al. 1987). Specifically, the alkalic-cap lavas range in SiO_2 from ~49% to 53% and lie well within the alkalic field on a total alkalis-SiO_2 plot (Fig. 3). They are dominantly hawaiites with rare mugearites; note that the trends for the Laupahoehoe and Hamakua lavas are offset in Fig. 4. In terms of normative components they contain approximately 70% feldspar and range from hypersthene normative (<10%) to slightly nepheline normative (<2.5%). With decreasing MgO content, CaO, FeO^T and TiO_2 contents systematically decrease and SiO_2, Al_2O_3, Na_2O, K_2O and P_2O_5 contents systematically increase (Fig. 5). Sample Mk-5 deviates from the general trend in K_2O, Al_2O_3 and P_2O_5. The largest decrease is for TiO_2 (~32%) and the largest increase is for P_2O_5 (~63%).

Trace elements. Abundances of the compatible elements Ni and Cr are very low, typically <10 ppm, and do not vary systematically with MgO content, probably because (1) these low abundance levels are near the detection limits and (2) some lavas are contaminated with Ni-rich, disaggregated dunite xenoliths. Sc abundances are also low, <15 ppm, and systematically decrease with decreasing MgO (Fig. 5b). The most dramatic trend is for V which decreases precipitously from 110 ppm in the most MgO-rich samples to ~30 ppm in the low MgO samples (Fig. 5b).

Abundances of the incompatible elements, Th, Zr, Hf, Nb and LREE vary positively with P_2O_5 (Fig. 6) and enrichment factors (most evolved lava/least evolved lava) are 1.42 to 1.56. Sr and Ba abundances are less variable. Sr abundances are high (1105 to 1134 ppm) and *decrease* with increasing P_2O_5 content. Ba is incompatible in these rocks

Table 2. Modal mineralogy of representative Laupahoehoe lavas. Modes (volume %) are based on 1000 point counts on each sample. Phenocrysts (ph) are >0.5 mm. Microphenocrysts (mph) are 0.1–0.5 mm

Sample	Olivine		Plagioclase		Magnetite		Ground-mass
	ph	mph	ph	mph	ph	mph	
Ml-2	–	0.7	–	0.6	–	0.3	98.4
Ml-3	–	0.2	–	0.9	–	–	98.9
Ml-20	–	0.1	–	0.2	–	0.3	99.4
Me-2	0.1	0.2	0.5	0.6	–	–	98.6
Me-6	–	0.1	1.4	0.2	0.1	0.4	97.8
Mk-1	–	0.1	0.3	0.3	–	0.7	98.6
Mp-1	–	–	0.6	1.0	0.1	0.8	97.5
Mi-3	–	–	–	–	–	0.9	99.1
Mi-5	0.2	–	–	–	–	–	99.8

Table 3. Microprobe analyses of minerals in Laupahoehoe Group lavas, Mauna Kea Volcano, Hawaii

Olivine

	Mi-2				Mi-5	
	mph	mph	mph	Xeno	mph	gm
SiO$_2$	37.78	37.65	38.07	38.27	38.86	37.71
FeO	22.74	22.91	23.11	17.99	17.75	24.16
MgO	39.25	39.55	38.90	43.30	43.55	37.75
Total	99.77	100.11	100.08	99.56	100.16	99.62
Fo%	75.5	75.5	75.0	81.1	81.4	73.6

Plagioclase

	Mi-2		Mi-5	
	ph	mph–0.15 mm	Xenocryst rounded–0.3 mm	mph–0.35 mm
SiO$_2$	53.66	53.40	49.86	53.40
Al$_2$O$_3$	29.26	29.44	32.21	29.65
FeO	0.59	0.76	0.51	0.65
CaO	11.40	11.55	14.47	11.56
Na$_2$O	4.44	4.28	2.94	4.26
K$_2$O	0.29	0.28	0.13	0.24
Total	99.64	99.71	100.22	99.76
An%	57.6	58.8	72.5	59.1

Fe-Ti Oxides

	Mi-2				Mi-5		
	mph 0.1 mm	mph 0.2 mm	mph 0.15 mm	gm	mph 0.1 mm	gm	Dunite beside
TiO$_2$	17.34	18.56	16.70	19.49	16.89	19.25	13.60
Al$_2$O$_3$	4.94	4.35	4.95	3.61	3.13	3.61	5.35
Cr$_2$O$_3$	0.00	0.04	0.03	0.05	1.85	0.04	6.50
FeO	68.34	68.90	67.67	67.07	67.47	67.47	63.83
MnO	0.55	0.70	0.65	0.74	0.64	0.67	0.21
MgO	4.70	4.52	5.55	4.52	5.89	5.07	6.44
Total	96.57	97.07	95.45	95.48	95.87	96.11	95.93
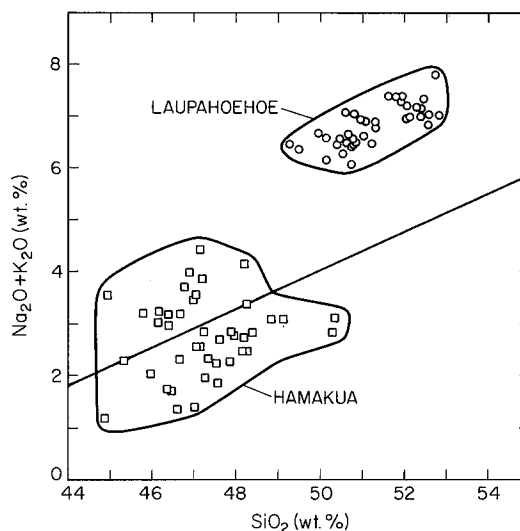
Fig. 3. Alkalis – SiO$_2$ plot for Mauna Kea lavas. Data for Hamakua shield lavas (Frey et al. 1988) straddle the tholeiitic-alkalic boundary (solid line from Macdonald and Katsura 1964), whereas the alkalic cap (Laupahoehoe Group) lavas lie well within the alkalic field. Note, there is no compositional overlap between shield lavas and these alkalic cap lavas
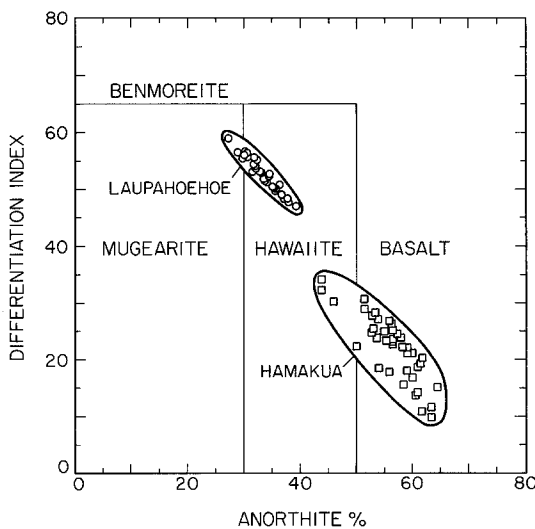
Fig. 4. Differentiation Index (DI = normative Q + Or + Ab + Ne + Ks + Lc) versus An% in normative plagioclase; a classification diagram from Coombs and Wilkinson (1969). The alkali cap is dominantly composed of hawaiites and distinct from the underlying shield lavas which range from basalt to hawaiite (Frey et al. 1988)

up to about 1.1 w% P$_2$O$_5$ (Fig. 6). Although most samples define coherent trends among incompatible element abundances, samples Mh-2 and Mh-4 have anomalously high P$_2$O$_5$ (e.g., P$_2$O$_5$ versus MgO, Ce, Ba and Nb). Sample Mk-6 has anomalously high Ba and sample Mk-5 has anomalously low K$_2$O and Rb (Figs. 5 and 6). Some of these geochemical deviations represent post-magmatic alteration processes; e.g., low K and Rb in Mk-5 probably reflects alkali mobility indicated by the occurrence of biotite in tension gashes.

REE abundances for the 19 samples analyzed span a narrow range and have significantly higher LREE/HREE ratios than the shield lavas; Eu anomalies are absent
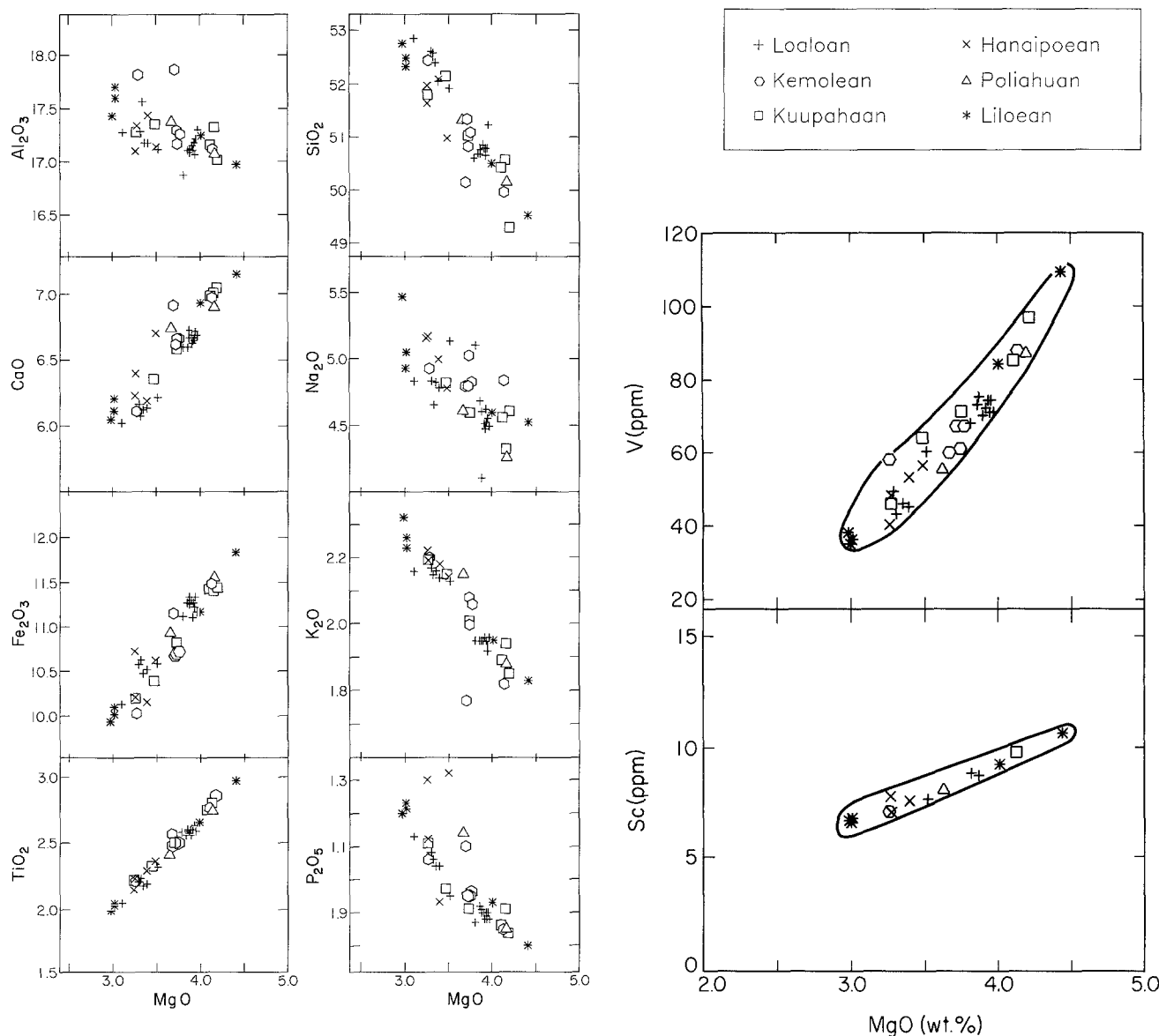
Fig. 5a. Major oxide – MgO variation diagram for Laupahoehoe lavas. Each time-stratigraphic group has a different symbol (legend in upper right panel); note coherent trend defined by samples; **b.** Abundances of the compatible elements, Sc and V, versus MgO for Laupahoehoe lavas

(Fig. 8). Within the alkalic cap lavas LREE/HREE ratios increase with decreasing MgO and increasing P_2O_5 (Liloean-Mi suite in Fig. 8a). La/Yb and Ce/Y (which is analogous to a LREE/HREE ratio) change by ~20% (Figs. 8 and 9).

Radiogenic isotopes. Sr, Nd and Pb isotopic data for 8 samples which span the age and the compositional range of Laupahoehoe lavas (Table 4) define a relatively restricted range which is slightly larger than analytical error, e.g. $^{87}Sr/^{86}Sr$ from 0.70335 ± 4 to 0.70351 ± 4. These small variations in isotopic ratios do not correlate with compositional variations or age. Sr, Nd and Pb isotopic ratios of Laupahoehoe lavas overlap with those of the underlying shield lavas (Table 4). However, the alkalic cap lavas trend to less radiogenic Pb ratios than the shield lavas. These results contrast with West Maui data where the alkalic cap lavas have slightly higher $^{206}Pb/^{204}Pb$ and $^{208}Pb/^{204}Pb$ ra-

tios than the shield lavas at comparable $^{87}Sr/^{86}Sr$ ratios (Hegner et al. 1986).

Discussion

Temporal and geographic compositional variations

The Laupahoehoe lavas show no consistent compositional variation with age or location. In particular, lavas within each of Porter's (1979) Laupahoehoe stage, including the Holocene unit which is common to both Porter's (1979) and Wolfe's (1987) subdivisions of the Laupahoehoe lavas, range widely in degree of differentiation (as measured by MgO content, incompatible trace element abundances and Al_2O_3/CaO) and in degree of silica saturation (as indicated by normative hypersthene and normative nepheline content; Fig. 9). The same is true for distance from the summit of the volcano. Over a 13.5 km distance from the summit,
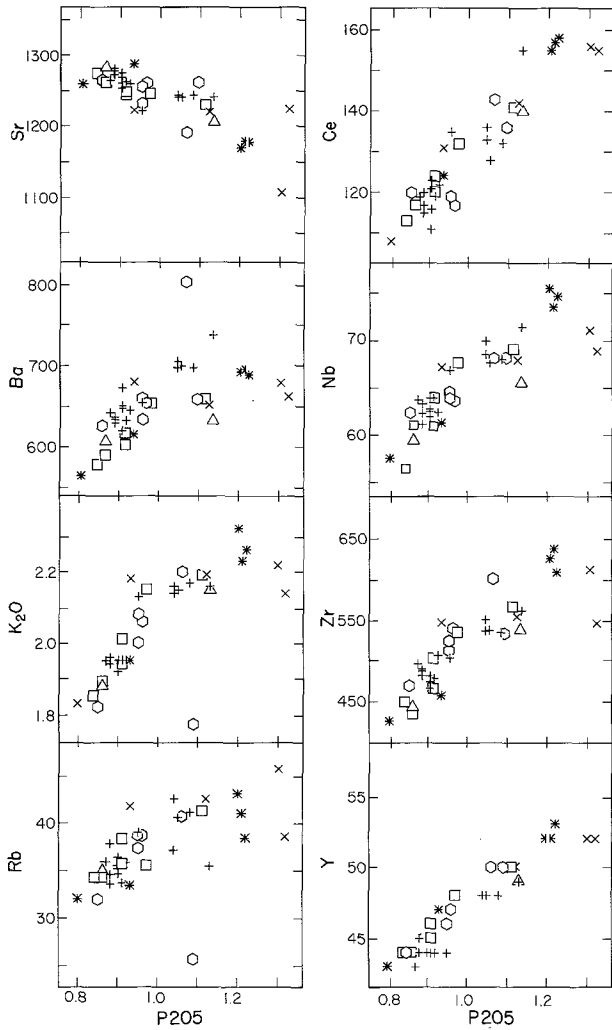
Fig. 6. Abundances of incompatible elements versus P_2O_5. Except for Sr, these elements are positively correlated with P_2O_5 content. Marked deviations from coherent trends are K_2O and Rb in Mk-5 which contains biotite in tension gashes and Ba which is inexplicably high in MK-6
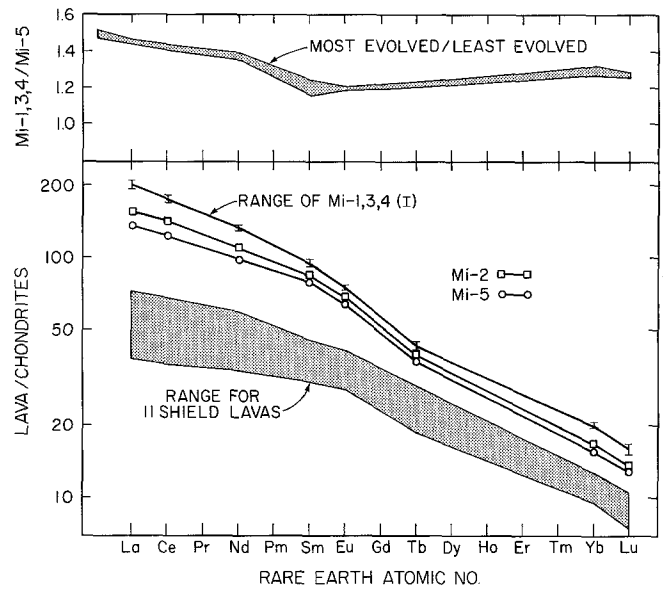

Fig. 7. Lower: Comparison of chondrite-normalized REE abundances in Hamakua shield lavas (range of 11 tholeiites and alkalic basalts from Maulua Gulch, Frey et al., 1988) to chondrite-normalized Laupahoehoe lavas. Data are shown for Liloean (Mi) series. The 14 other Laupahoehoe lavas (Table 1) fall within the range of the Mi samples.

Upper: REE in evolved Laupahoehoe hawaiites (Mi 1, 3, 4) compared to the least evolved hawaiite (Mi 5). Note the convex downward pattern

there is an elevation change of over 2.2 km. Despite this significant difference in elevation, there is no correlation of composition of the Laupahoehoe lavas with distance from the summit (elevation). In contrast, there is a strong correlation of vent location (i.e. proximity to the summit) with composition at Mauna Loa and Kilauea volcanoes. This correlation is interpreted as reflecting shallow reservoir systems (e.g., Wright and Fiske 1971; Rhodes 1987).

Compositional variation among
Mauna Kea alkalic cap lavas:
evaluation of a fractional crystallization model

Given the small variations in radiogenic isotopic ratios (Table 4) and coherence in the abundance trends (Figs. 5 and 6), it is probable that the compositional trends of the Laupahoehoe lavas were dominantly controlled by a relatively simple process such as fractional crystallization. The geochemical data can be used to develop and evaluate a fractional crystallization model. Following, are geochemical constraints on the fractionating mineral assemblage.

Fig. 8. Ce/Y and Al_2O_3/CaO versus MgO. Ce/Y correlates positively with La/Yb. Therefore, the plot shows increasing fractionation of REE as MgO decreases. These trends require an important role for clinopyroxene fractionation
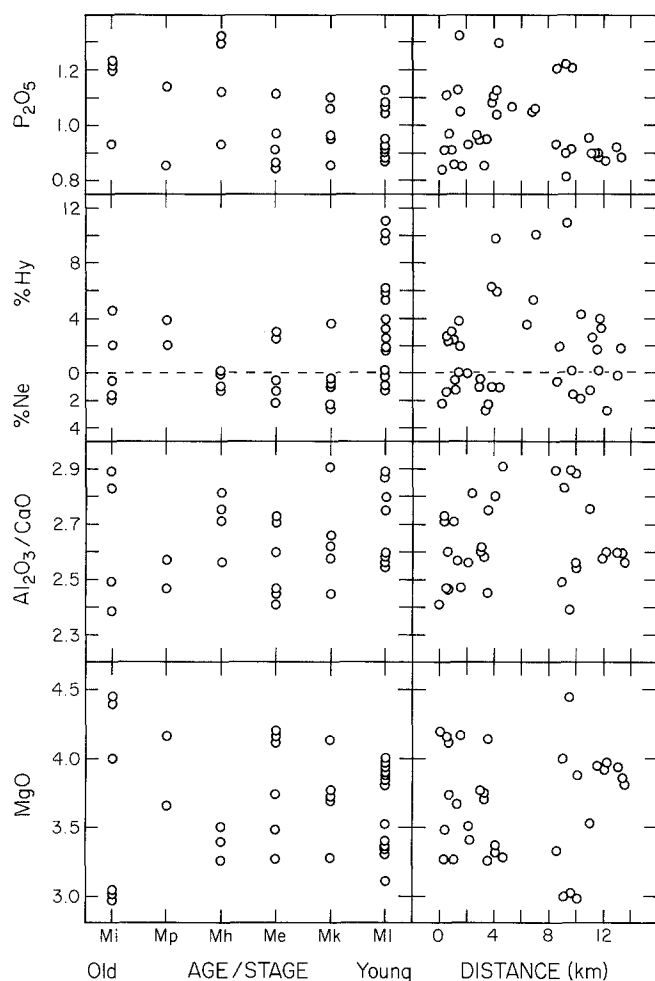
Fig. 9. Variation in the composition of Laupahoehoe Group lavas as a function of age and distance from the summit of Mauna Kea. No correlations are evident for incompatible (P_2O_5) or compatible (MgO) elements, Al_2O_3/CaO ratio or degree of silica saturation (normative %Hy or Ne)

1) The very low Ni and Cr abundances and Mg/Fe ratios require fractionation of mafic phases such as olivine, spinel and pyroxene;

2) The systematic increase in Al_2O_3/CaO with decreasing MgO (Fig. 8) requires a significant role for clinopyroxene. Clinopyroxene fractionation also could explain the increase in La/Yb and Ce/Y and decrease in Sc with decreasing MgO content (Figs. 5, 7 and 8).

3) The compatible behavior of Sr (Fig. 6) requires plagioclase fractionation.

4) The marked decrease in TiO_2 and V with decreasing MgO (Fig. 6) requires segregation of Fe-Ti oxides. Because Nb is more compatible than Zr in Fe-Ti oxides (e.g., McCallum and Charette, 1978; Pearce and Norry, 1979), the decreases in Nb/Zr and Nb/La with decreasing MgO are also consistent with significant fractionation of Fe-Ti oxides.

5) The inverse relation between MgO and SiO_2 (Fig. 6) requires subtraction of SiO_2-poor phases such as olivine and Fe-Ti oxides.

6) The incompatible behavior of P_2O_5 (0.80 to 1.32%) and absence of apatite as phenocrysts or microphenocrysts suggest that apatite was not a fractionating phase. This is consistent with the apatite-saturation equation proposed by Harrison and Watson (1984); i.e. $\sim 2\%$ P_2O_5 is needed to reach apatite saturation in a hawaiite melt at 1100 °C.

The petrographic characteristics of Laupahoehoe lavas are also important in evaluating a fractional crystallization model; e.g., their nearly-aphyric nature establishes that each analysis is representative of a melt, and the scarcity of phenocrysts requires very efficient segregation of postulated fractionating phases. However, the rare presence of olivine and plagioclase xenocrysts that crystallized from melts less evolved than the most mafic hawaiites (Tables 2 and 3) may provide evidence for a range of magma compositions along a liquid line of descent. The absence of clinopyroxene despite geochemical trends requiring clinopyroxene fractionation (Figs. 5, 7 and 8) is another example of a "clinopyroxene paradox" (e.g., Dungan and Rhodes, 1978).

Table 4. Radiogenic isotope data for Laupahoehoe lavas

Samples	$^{87}Sr/^{86}Sr$	$^{143}Nd/^{144}Nd$	$^{206}Pb/^{204}Pb$	$^{207}Pb/^{204}Pb$	$^{208}Pb/^{204}Pb$
Youngest					
Ml-2[a]	0.70349 ± 4	0.513054 ± 13	18.321	15.456	37.894
Ml-11	0.70349 ± 4				
Ml-19	0.70338 ± 4	0.513070 ± 40			
Mk-6	0.70350 ± 4	0.513004 ± 18	18.358 ± 17	15.478 ± 15	37.952 ± 37
	0.70350 ± 5				
Me-6	0.70343 ± 4	0.513018 ± 30	18.332 ± 16	15.468 ± 14	37.914 ± 35
Mh-4[a]	0.70342 ± 4	0.512973 ± 30	18.324	15.430	37.870
Mp-1[a]	0.70351 ± 4	0.513016 ± 19	18.339	15.460	37.946
Oldest					
Mi-5	0.70335 ± 4	0.513033 ± 20	18.322 ± 5	15.463 ± 5	37.907 ± 11
Range for 10	0.70346	0.513008	18.36	15.44	37.887
Hamakua Lavas	to	to	to	to	to
(Frey et al. 1988)	0.70361	0.513053	18.44	15.55	38.069

[a] Mean of 2 Pb analyses

Sr and Nd data with two sigma uncertainty determined at MIT by Kennedy
Pb data determined by S.-T. Kwon at Univ. Calif. Santa Barbara.
Reproducibility is better than 0.08% per mass unit for $^{204}Pb/^{206}Pb$ and 0.05% for $^{207}Pb/^{206}Pb$ and $^{208}Pb/^{206}Pb$

In order to quantitatively evaluate fractional crystallization as a major process in controlling compositional variations within the Laupahoehoe Group, we modelled compositional variations within several of the Laupahoehoe stages, including the Holocene unit. Similar results were obtained for each stage. We discuss in detail modelling for the oldest group (Liloean, Mi-1 through Mi-5) because it has the largest compositional range. Sample Mi-5 is the least evolved Laupahoehoe lava. Samples Mi-1, Mi-3 and Mi-4 are among the most evolved and sample Mi-2 is intermediate.

Major element modelling. There is little experimental information about equilibrium mineral compositions for hawaiite melts as a function of pressure and temperature; consequently, we have not evaluated major element trends during fractional crystallization or small increments of equilibrium crystallization (e.g., Grove and Baker 1984). Rather we used a least squares approach assuming equilibrium crystallization to model major element variations among the Mi samples. Undoubtedly the fractionation process is more complex, but over the compositional range (4.4–3.0% MgO) of the hawaiites this approach should be adequate for determining the nature and proportions of fractionating phases.

Compositional variations within the Mi series were modelled in steps: Mi-5 to Mi-2, Mi-2 to Mi-3, and as a single step of Mi-5 to Mi-3 or Mi-1. In each case mineral compositions were chosen to have Fe/Mg ($K_D = 0.3$ for olivine, ~ 0.25 for cpx) and Ca/Na ($K_D \sim 1.5$–1.7 for plag.) in equilibrium with the evolved melt.

For the Mi-5 to Mi-2 step two sources of olivine, plagioclase and oxide data were used: (a) microphenocryst compositions in Mi-2 (Table 3) and (b) compositions typical of minerals in Fe-Ti oxide-rich, gabbroic xenoliths in these hawaiites (Fodor and Van der Meyden, 1988). These xenoliths are interpreted by Fodor and Van der Meyden (1988) as cumulates from Mauna Kea magmas. The evolved composition of the minerals in these xenoliths indicates that they may have formed during crystal fractionation of hawaiite melts. These oxide-rich gabbros contain ilmenite and clinopyroxene. Both are absent as xenocrysts or microphenocrysts in Laupahoehoe lavas. As discussed above, clinopyroxene is required as a fractionating phase if these hawaiites are genetically related. Because clinopyroxene (cpx) is not a phenocryst or microphenocryst phase in the Laupahoehoe lavas, its composition is the largest uncertainty in the modelling. Three different approaches were used to estimate cpx compositions:

1) It is known that the stability field for cpx in basic melts expands with increasing pressure (e.g., Mahood and Baker 1986). Therefore, the geochemical evidence in Laupahoehoe lavas for clinopyroxene fractionation may reflect moderate pressure crystallization. Specifically, for hawaiites experimental studies have found that cpx is the liquidus phase only at moderate to high pressures ≥ 8 kb (Thompson 1974; Knutson and Green 1975; Mahood and Baker 1986). We used the results of Mahood and Baker to estimate clinopyroxene composition in equilibrium with hawaiite melts at 8 kb (for details see model 1 A in Table 5).

2) Ankaramites occur in the uppermost portion of the Mauna Kea shield. These cpx-rich rocks probably formed in part by clinopyroxene accumulation (Frey et al. 1988).

We used clinopyroxene from an ankaramite for model 1 B (Table 5).

3) Clinopyroxene and Fe-Ti oxide-bearing gabbroic xenoliths are common in Mauna Kea hawaiites (Jackson et al. 1982: Fodor and Van der Meyden 1988). Compositions of clinopyroxene, plagioclase and Fe-Ti oxides in these gabbros were used in the fractionation models (model 2 of Table 5). Clinopyroxene in these gabbros is significantly less aluminous than other clinopyroxene compositions used in modeling (Table 5).

These estimates of the fractionating clinopyroxene composition vary considerably and enable evaluation of the sensitivity of the models to choice of clinopyroxene composition. The fractionating assemblages used to model the small compositional step from Mi-5 to Mi-2 (4.42%–4.01% MgO) all yield acceptable fits to the data with similar degrees of fractionation, 7.2–8.6% (Table 6). Except for K_2O all oxides are fit within analytical error. The calculated K_2O is 5–7% too low. This could be explained by fractionation of a more potassium-rich feldspar, by derivation from a parent with a lower K_2O content or late-stage K_2O mobility. All models require plagioclase as the dominant fractionating phase with olivine, magnetite and ilmenite in decreasing abundance. Exclusion of ilmenite as a fractionating phase results in poor mass balances for TiO_2. Fodor and Van der Meyden (1988) identified two types of gabbroic xenoliths, olivine-gabbro and opaque-rich gabbro, in Mauna Kea hawaiites. The latter group has model proportions very similar to the calculated fractionating assemblage (Table 6). In particular, the calculated abundance of Fe-Ti oxides (~ 15–20 wt.% of the crystallizing assemblage) is in excellent agreement with the high proportion (11–27 vol.%) of Fe-Ti-oxides in the opaque-rich gabbroic xenoliths.

Models for the step of Mi-2 to Mi-3 and the sum of two steps Mi-5 to Mi-2 plus Mi-2 to Mi-3 were evaluated also. Results of the two step model are very similar to the single step from Mi-5 to Mi-3 (Table 6b). This single step encompasses almost the largest compositional variation among the hawaiites (4.42–3.01% MgO). The compositional change from Mi-5 to Mi-3 was also satisfactorily modelled with a fractionating assemblage of plagioclase > clinopyroxene > Fe-Ti oxides > olivine, but this step requires considerably more fractionation, $\sim 27\%$ (Table 6). Again, the high wt.% of oxides ($\sim 16\%$ of the crystallizing assemblage) in these models corresponds to that in the opaque-rich gabbros. We also modelled the evolution of sample Mi-1 from Mi-5. Because Mi-1 is slightly more evolved than Mi-3 (Table 1), this model requires slightly more fractionation, $\sim 30\%$ (Table 6).

Because the major element discrepancies are small, crystal-melt segregation is a viable process to explain the major element abundance trends among the Liloean (Mi) samples. An unanticipated major conclusion is that the fractionating assemblage contained substantial amounts of clinopyroxene and Fe-Ti oxides. The important role of clinopyroxene (18–26%) is surprising in that it does not occur as a phenocryst or microphenocryst in these nearly aphyric hawaiites. A possible explanation is that the small amounts of plagioclase and olivine phenocrysts and microphenocrysts in Laupahoehoe lavas (Table 2) reflect low pressure crystallization and that fractionation of a clinopyroxene-bearing assemblage occurred at moderate pressures. Experimental studies of hawaiite compositions clearly show that the clinopyrox-

Table 5. Mineral compositions for crystal fractional models. Models: *1a* – equilibrium minerals calculated using K_D's listed (cpx composition from Mahood and Baker, 1986); 1b – as in model 1a except cpx from a Mauna Kea ankaramite, C-74; 2-minerals in cumulate gabbro xenoliths in Laupahoehoe hawaiite (Fodor and Van der Meyden 1988)

Daughter	Mi-2						Mi-1, 2, 3			
Model	1a, 1b, 2	1a, 1b	2	1a	1b	2	1a, 1b		2	
Mineral	Oliv	Plag	Plag	Cpx	Cpx	Cpx	Magt	Ilm	Magt	Ilm
Oxide										
SiO_2	37.58	53.71	54.83	48.36	48.40	48.9	–	–	–	–
TiO_2	–	–	–	1.99	2.44	1.4	20.00	52.85	18.82	50.17
Al_2O_3	–	29.52	28.75	8.72	6.11	3.5	4.52	0.17	2.45	0.39
FeO	22.68	0.76	0.32	6.97	7.26	9.0	71.52	42.92	75.05	45.03
MgO	39.14	–	–	13.22	13.75	14.4	4.69	4.94	4.03	6.23
CaO	0.25	11.58	10.64	20.00	21.85	21.3	–	–	–	–
Na_2O	–	4.29	4.87	0.74	0.30	0.4	–	–	–	–
K_2O	–	0.28	0.30	–	–	–	–	–	–	–
Comments	Fo 75.5 $K_D=0.27$	An 59.1 $K_D=1.79$	An 54.1	$K_D=0.25$			from Mi-2	from Ki-12		

Daughter	Mi-1, 3					
Model	1a, 1b, 2	1a, 1b	2	1a	1b	2
Mineral	Oliv	Plag	Plag	Cpx	Cpx	Cpx
Oxide						
SiO_2	37.46	54.72	54.83	48.10	48.60	49.66
TiO_2	–	–	–	1.53	2.45	1.29
Al_2O_3	–	27.95	28.75	8.88	6.08	3.29
FeO	26.95	0.79	0.32	8.05	8.31	9.03
MgO	35.26	–	–	12.62	13.04	14.14
CaO	0.25	10.18	10.64	20.00	21.75	21.90
Na_2O	–	5.40	4.87	0.82	0.35	0.42
K_2O	–	0.52	0.30	–	–	–
Comments	Fo 70 $K_D=0.30$	An 49.5 $K_D=1.54$	An 53.7 $K_D=1.78$	$K_D=0.25$		

Table 6. Results of crystal fractionation modeling using minerals and models from Table 5. Sign of residuals (+or–) is the difference between observed minus calculated for the parent lava, Mi-5. R^2 is the sum of the residuals squared

Residuals											Fractionation Assemblage					
Daughter	Model	SiO_2	TiO_2	Al_2O	FeO	MgO	CaO	Na_2O	K_2O	R^2	Plag	Cpx	Oliv	Magt	Ilm	Residual melt
Mi-2	1a	−0.01	0.00	0.00	0.00	0.00	0.01	0.03	0.01	0.001	2.7	1.9	1.0	1.0	0.5	92.8
	1b	−0.01	0.00	0.00	0.00	0.01	0.01	0.03	0.01	0.001	3.0	1.6	1.1	1.0	0.5	92.8
	2	−0.01	0.00	0.00	0.00	0.01	0.01	0.03	0.02	0.001	4.0	1.7	1.2	1.0	0.7	91.4
Mi-3	1a	−0.02	0.00	0.02	0.00	0.02	0.02	0.04	0.12	0.018	12.5	6.7	3.4	2.5	1.7	73.2
	1b	−0.02	0.00	0.02	0.00	0.02	0.03	0.04	0.13	0.020	13.8	5.7	3.8	2.6	1.7	72.4
	2	−0.03	0.00	0.03	0.00	0.03	0.04	0.09	0.16	0.038	14.2	5.1	3.7	2.3	2.1	72.6
Mi-1	1a	−0.01	0.00	0.03	0.00	0.01	0.00	−0.08	0.14	0.028	14.8	7.2	3.6	2.8	1.8	69.8
	1b	−0.01	0.00	0.03	0.00	0.01	0.01	−0.08	0.15	0.031	16.2	6.2	3.9	2.9	1.7	69.1
	2	−0.02	0.00	0.03	0.00	0.02	0.03	−0.02	0.18	0.037	16.6	5.5	3.9	2.6	2.2	69.2

ene stability field increases with increasing pressure (Thompson 1974; Knutson and Green 1975; Mahood and Baker 1986).

The major element trends of the alkalic cap lavas are consistent with crystal fractionation at moderate pressures.

Specifically, in a projection onto the olivine-clinopyroxene-nepheline plane these lavas define a coherent trend displaced from the low pressure cotectic (Fig. 10). The coherency of the trend supports the interpretation that Laupahoehoe lavas are genetically related and the offset from
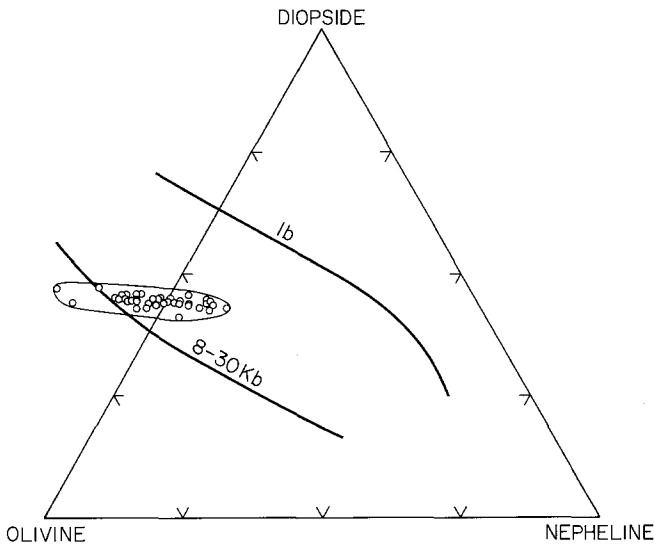
Fig. 10. Major oxide compositions of Laupahoehoe hawaiites projected from plagioclase onto the olivine-diopside-nepheline plane following the convention of Sack et al. (1987). The hawaiite trend is coherent but plots to the high pressure side of the 1 bar olivine-clinopyroxene-plagioclase cotectic detemined by Sack et al. (1987)

the 1 bar cotectic is consistent with fractionation occurring at moderate pressures. Moderate pressure fractionation does not explain the absence of clinopyroxene in the lavas but two possibilities are resorption of clinopyroxene during ascent or that crystallization occurred only along wall-rock boundaries of the magma body.

We cannot closely constrain the depth of fractionation but a minimum pressure estimate can be made from the densities of CO_2 inclusions in dunite xenoliths. Dunite xenoliths are commonly found in Hawaiian alkalic cap lavas (Clague 1987) and they occur in some Laupahoehoe lavas (Jackson et al. 1982). There are no compositional or age differences between Laupahoehoe lavas with and without dunite xenoliths. We conclude that the presence of these xenoliths are related to the eruption process. However, the xenoliths are useful for estimating minimum depths for formation of the Laupahoehoe hawaiites. From studies of CO_2 fluid inclusions in several Hawaiian dunite xenoliths, including a dunite from Mauna Kea, Roedder (1965, 1976)

and Murck et al. (1978) infer minimum trapping pressures of 2.2–5 Kb. We infer that after incorporation of dunite xenoliths the Mauna Kea alkalic cap lavas ascended rapidly from *at least* depths corresponding to these minimum pressure estimates. However, this inference is tentative because a detailed study of dunite xenoliths in Mauna Kea lavas has not been completed. We recently initiated such a study in collaboration with E. Roedder.

Trace element modelling. Because abundances of 8 major elements were modelled with 6 phases including melt, it is not surprising that mathematically reasonable models were obtained. Therefore, it is important to use trace element abundances as an independent test of the major-element based fractionation models. Because of uncertainties in trace element partition coefficients for minerals in equilibrium with evolved alkalic melts (e.g., Lemarchand et al. 1987), abundances of compatible and moderately incompatible elements were not quantitatively modelled. Nevertheless, trace element abundances in the hawaiites provide strong evidence for each of the major fractionating phases required by the major element abundance trends. This is most clearly illustrated by comparing trace element abundance ratios between evolved hawaiites and less-evolved hawaiites; e.g., samples Mi-1, 3 and 4 relative to Mi-5 (Fig. 11). The order of increasing enrichment, i.e. incompatibility, is not that observed among oceanic basalts (e.g., Bougault et al. 1984, 1985), or in basalt/primitive mantle ratios (e.g., Wood 1979; Sun 1980). The ordering of enrichment factors in Laupahoehoe lavas reflects fractionation of plagioclase, clinopyroxene and Fe-Ti oxides. Specifically, the relative compatibility of Ba, Rb, K and Sr is consistent with segregation of plagioclase with a significant alkalic component (e.g., Philpotts and Schnetzler 1970); the higher compatibility of Nb relative to Zr together with the V depletion strongly indicates the segregation of Fe-Ti oxide phases (Pearce and Norry 1979; Shervais 1982; Lemarchand et al. 1987), and the decrease in Sc content with increasing differentiation requires clinopyroxene and/or Fe-Ti oxide fractionation. For example, the Sc and V variation from Mi-5 to Mi-3 (Fig. 5) require bulk-solid/melt partition coefficients of 2.5 and 4.6, respectively, for 27% fractionation (Table 6). While these values require large partition coefficients for clinopyroxene and Fe-Ti oxides which comprise ~40% of the fractionating assemblage (Table 6), the in-
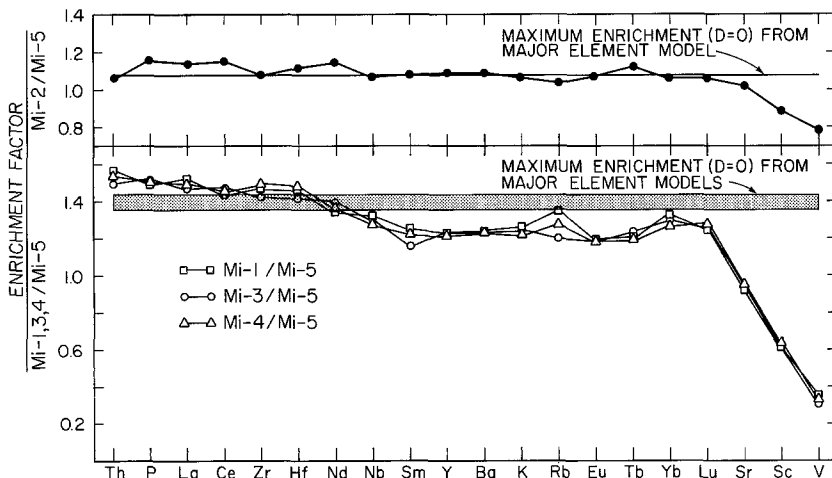

Fig. 11. *Upper*: Trace element enrichment factors for an intermediate composition hawaiite, Mi-2, relative to a mafic hawaiite, Mi-5. Elements arranged in approximate order of enrichment. *Solid line* indicates maximum enrichment expectd for a totally incompatible element $(D = O)$ based on major element models in Table 5b. *Lower*: Enrichment factors for evolved hawaiites, Mi-1, 3 and 4 relative to Mi-5. *Solid line* indicates maximum enrichment expected for a totally incompatible element based on major element models in Tables 6b and 6c. Note the excess enrichment of the most incompatible elements, Th, P and La. Identical enrichments are present for lavas from other age groups

ferred mineral/melt partition coefficients are within the observed range (cf. Shervais 1982; Lemarchand et al. 1987).

The lack of an Eu anomaly in the hawaiites (Fig. 7) and the disparate behavior of Sr and Eu, i.e., Sr abundance decreases with differentiation but Eu abundance increases (Fig. 11) require that most of the Eu was Eu^{+3}; hence a relatively high oxygen fugacity is inferred. High oxygen fugacities are also reflected by high Fe_2O_3/FeO ratios, typically 0.45, of the lavas, although the variability of this ratio (Table 1) probably reflects late-stage oxidation during cooling.

The trace element systematics of these lavas provide evidence that the crystal fractionation process was not simple closed system fractional or equilibrium crystallization. For example, enrichment factors for highly incompatible elements (Th, P, La Ce) in the Mi group are 1.44–1.56 which exceeds the maximum enrichment of 1.36–1.45 (D = O) from major element models (Fig. 11). Furthermore, the convex downward REE patterns of the evolved hawaiites (samples Mi-1, 3, 4) relative to the more mafic hawaiite Mi-5 (Fig. 7a) are enigmatic. Although fractionation of apatite (Watson and Green 1981) and/or amphibole (Irving and Frey, 1984) could produce this pattern, these phases were not involved in the transition from mafic to evolved hawaiite. Neither phase occurs in the lavas. Furthermore, P is a highly incompatible element in these lavas (Fig. 6 and 11). Hofmann et al. (1987) invoked clinopyroxene fractionation to explain similar REE abundance trends in Kohala lavas (which contain modal apatite; Spengler and Garcia, 1988). During fractional crystallization changes in abundances ratios reflect absolute differences in partition coefficients; i.e.,

$$\frac{(C_A/C_B)_{\text{residual melt}}}{(C_A/C_B)_{\text{initial melt}}} = F^{D_A - D_B}$$

(C and D indicate concentrations and bulk-solid/melt partition coefficients for elements A and B). Thus, the 22% increase in La/Sm from Mi-5 to the evolved hawaiites requires $(D_A - D_B) = -0.57$ for 30% crystallization (Table 6). (A similar value results from a total equilibrium model). Therefore, if D_{La} is assumed to be zero, then $D_{Sm}^{cpx/melt} = 2.3$ if cpx is the only phase controlling REE fractionation. Because cpx/melt partition coefficients for Sm are typically less than unity for melts with ~50% SiO_2 (e.g., Green and Pearson 1985; Lemarchand et al., 1987), the closed system fractionation model may be incapable of explaining the extent of REE fractionation among the hawaiites (Fig. 7).

An additional trace element complexity is the limited enrichment of K, Rb and Ba during fractionation (Fig. 11). Using the major element model results (Table 6) we infer that plagioclase had partition coefficients of ~0.8 for K, Rb and Ba and ~2.4 for Sr. This Sr value is typical for the plagioclase (An_{50-60}) used in the major element modelling but such high partition coefficients for K, Rb, and Ba are typical of more alkalic feldspars (An < 40) formed in silicic magmas (e.g., Nash and Crecraft 1985).

Within the context of a fractional crystallization model the described trace element complexities can be explained by several alternatives:

1) The simplest possibility is that partition coefficients for clinopyroxene and plagioclase coexisting with hawaiite melts are significantly larger than in basaltic systems. However, this possibility is not supported by clinopyroxene and plagioclase partition coefficients for hawaiite melts from the Azores (Lemarchand et al. 1987). Moreover, this alternative would accentuate the excess incompatible element enrichment which is not explained by the closed system model (Figure 11).

2) It is also possible that individual Laupahoehoe hawaiites evolved from basaltic parents formed by different degrees of melting. If these parents were similar in major element composition but differed in incompatible element contents, the Laupahoehoe data set could be explained.

3) Another possibility is that the fractionation was polybaric, perhaps plagioclase, olivine and clinopyroxene fractionation at moderate pressures and plagioclase, olivine and oxide fractionation at lower pressures. Single step models may only average the effect of multiple or continuous fractionation events at different pressures. If this complex model is more realistic, modelling based on a simpler single-stage process is likely to result in inconsistencies.

4) The hawaiites may have formed in a periodically replenished magma chamber with mixing between less evolved recharge magmas and more evolved magmas formed by fractional crystallization in the magma chamber. This process can decouple major and trace element behavior (O'Hara and Matthews 1981). The presence of rare disequilibrium xenocrysts might reflect magma mixing.

5) An alternative complex crystallization model which could explain features of the hawaiite data not explained by closed system fractionation is the recently proposed model for crystallization of a magma chamber through in situ crystallization in a boundary layer (Langmuir 1986, 1988). The boundary layer which is cooling and partially crystallizing is maintained in a steady state by input melt from the main magma and return of residual melt to the convecting magma system where it is mixed. This model yields important differences from conventional models of magma crystallization because the precipitated solids are only in equilibrium with residual melt in the layer and not with the entire magma mass. Therefore, geochemical imprints of late-crystallizing phases can be imparted to magma in the main chamber because of the high degree of crystallization occurring in the crystallizing layer which returns residual melt to the main magma mass.

Because there are insufficient experimental data for defining major and trace element abundance trends on liquid lines of descent for hawaiite melts at various pressures, we are not able to confidently choose between these alternative complexities. However, the presence of dense xenoliths in the hawaiite lavas probably precludes evolution of the hawaiites in a long-lived, shallow magma chamber. We suspect that much of the crystal-melt segregation occurred on conduit or magma chamber walls. Mafic layers in alpine peridotites provide abundant evidence for crystallization along conduit walls (e.g., Bodinier et al. 1987; Kornprobst and Piboule 1987; Suen and Frey 1987). If crystallization is restricted to walls of conduits or magma chambers this may also be an explanation for the commonly aphyric nature of low MgO lavas on oceanic islands (Maaloe et al. 1986); i.e., the Mauna Kea hawaiites were erupted from the more voluminous crystal-free central portion of the magma chamber or associated conduits.

Summary

The alkalic cap, Laupahoehoe Group, of Mauna Kea volcano is composed exclusively of evolved lavas, dominantly

hawaiites with less than 4.5% MgO. They were erupted over the last 65000 years. There are no obvious correlations of lava compositions, including radiogenic isotope ratios, with eruption age or location. However, a suite of 39 samples shows substantial and coherent major and trace element abundance variations. The well-defined major element abundance trends and compatible behavior of Sr can be explained by crystal-melt fractionation models involving up to 30% segregation of a cumulate formed of $\sim 50\%$ plagioclase plus major amounts of clinopyroxene and Fe-Ti oxides with minor olivine. A complexity to this fractionation model is that clinopyroxene is not a xenocryst or phenocryst in Laupahoehoe lavas. However, if these lavas are related, clinopyroxene segregation is *required* to explain geochemical trends such as decreasing Sc and CaO/Al_2O_3 with increasing differentiation (Fig. 8). Moderate, 2–5 kb, pressure fractionation is proposed as the explanation of this "clinopyroxene paradox". This is consistent with (a) experimental studies showing expansion of the clinopyroxene field in basaltic and hawaiite melts with increasing pressure (e.g. Thompson 1974; Mahood and Baker 1986), (b) occurrence within the hawaiites of clinopyroxene and Fe-Ti oxide-rich gabbroic xenoliths which Fodor and Van der Meyden (1988) interpret as cumulates, and (c) occurrence within the hawaiites of dunite xenoliths with CO_2 inclusions in olivine having densities which require trapping at minimum pressures of 2 kb.

Although closed system fractional crystallization of a magma chamber at moderate pressure explains most of the geochemical trends, we suggest that intra-hawaiite evolution was polybaric and involved crystallization on conduit or magma chamber walls. Evidence for these complexities are:

1) The nearly aphyric texture of the hawaiites, the rare presence of olivine and plagioclase xenocrysts and the absence of clinopyroxene phenocrysts or xenocrysts contrast with the geochemical data which require a moderate pressure stage where clinopyroxene was an important fractionating phase.

2) The dense dunitic and Fe-Ti oxide-rich gabbroic xenoliths which are common in these lavas are unlikely to have remained suspended in a magma chamber (Clague, 1987).

3) There is a small but significant (~ 5–10%) decoupling between major and incompatible trace element abundances.

4) Within each of the six time-stratigraphic stages of the Laupahoehoe Group there are significant compositional variations, but there is no overall temporal variation. Consequently, these compositional changes occurred within a single magmatic system on the scale of a few thousand years or the lavas formed in many isolated magmatic systems.

A model of crystal segregation along conduit walls over a range in pressure is consistent with the compositional variations of the alkalic cap lavas at Mauna Kea.

References

Bargar KE, Jackson ED (1974) Calculated volumes of individual shield volcanoes along the Hawaiian-Emperor chain. USGS J Res 2:545–550

Bodinier JL, Guiraud M, Fabries J, Dostal J, Dupuy C (1987) Petrogenesis of layered pyroxenites from the Lherz, Freychinede and Prades ultramafic bodies (Ariege, French Pyrenees). Geochim Cosmochim Acta 51:279–290

Bougault H, Joron JL, Treuil M (1984) Mantle heterogeneity: Along strike variations of hygromagmaphile elements between Azores and 10 °N. Proc 27th Int Geol Congr, Moscow

Bougault H, Joron JL, Treuil M, Maury R (1985) Local versus regional mantle heterogeneities: evidence from hygromagmaphile elements. Init Rept DSDP 82, pp 459–482

Clague DA (1987) Hawaiian alkaline volcanics. In: JG Fitton et al. (eds) Alkaline igenous rocks; Geological society special publications 30. Blackwell, Oxford Boston Victoria, pp 227–252

Coombs DS, Wilkinson JFG (1969) Lineages and fractionation trends in undersaturated volcanic rocks from the East Otago volcanic province (New Zealand) and related rocks. J Petrol 10:440–501

Dungan MA, Rhodes JM (1978) Residual glasses and melt inclusions in basalts from DSDP Legs 45 and 46: evidence for magma mixing. Contrib Mineral Petrol 67:417–431

Dzurisin D, Koyanagi RY, English TT (1984) Magma supply and storage at Kilauea Volcano, Hawaii, 1956–1983. J Volcanol Geotherm Res 21:177–206

Feigenson MD, Spera FJ (1981) Dynamical model for temporal variation in magma type and eruption interval at Kohala Volcano, Hawaii. Geology 9:531–533

Fodor RV, Van der Meyden HJ (1988) Petrology of gabbroic xenoliths from Mauna Kea Volcano, Hawaii. J Geophys Res 93:4435–4452

Frey FA, Kennedy A, Garcia MO, Wise WS, Kwon ST, West HB (1987) Evolution of Mauna Kea Volcano, Hawaii. In: Abstr volum, Hawaii Symp on How Volcanoes Work, Hilo. Hawaii, p 81

Frey FA, Wise WS, Garcia MO, Kennedy A, Kwon, ST, West H (1988) Evolution of Mauna Kea Volcano, Hawaii: the transition from shield building to the alkalic cap stage. Contrib Mineral Petrol

Garcia MO, Frey FA, Grooms DG (1986) Petrology of volcanic rocks from Kaula Island, Hawaii: Implications for the origin of Hawaiian phonolites. Contrib Mineral Petrol 94:461–471

Green TH, Pearson NJ (1985) Rare earth element partitioning between clinopyroxene and silicate liquid at moderate to high pressure. Contrib Mineral Petrol 91:24–36

Grove TL, Baker MB (1984) Phase equilibrium controls on the tholeiitic versus calc-alkaline differentiation trends. J Geophys Res 89:3253–3274

Grunenfelder MH, Tilton GR, Bell K, Blenkinsop J (1986) Lead and strontium isotope relationships in the Oka Carbonatite Complex, Quebec. Geochim Cosmochim Acta 50:461–468

Harrison TM, Watson EB (1984) The behavior of apatite during crustal anatexis: Equilibrium and kinetic considerations. Geochim Cosmochim Acta 48:1467–1477

Hart SR, Brooks C (1977) The geochemistry of Early Precambrian mantle. Contrib Mineral Petrol 61:109–128

Hegner E, Unruh D, Tatsumoto M (1986) Nd-Sr-Pb isotope constraints on the sources of West Maui Volcano, Hawaii. Nature 319:478–480

Hofmann AW, Feigenson MD, Raczek I (1987) Kohala revisited. Contrib Mineral Petrol 95:114–122

Ila P, Frey FA (1984) Utilization of neutron activation analysis in the study of geologic materials. Atomkernenergie Kerntechnik 44:710–716

Irving AJ, Frey FA (1984) Trace element abundance in megacrysts and their host basalts: Constraints on partition coefficients and megacryst genesis. Geochim Cosmochim Acta 48:1201–1221

Jackson ED, Beeson MH, Clague DA (1982) Xenoliths in volcanic rocks from Mauna Kea Volcano, Hawaii. USGS Open File Report 88–201, 19 pp

Klein FW (1982) Patterns of historical eruptions at Hawaiian volcanoes. J Volcanol Geoth Res 12:1–35

Kornprobst J, Piboule M (1987) Igneous layering and crypto-layering in corundum-bearing garnet pyroxenite (grospydite) from the Beni Bousera ultramafic body. Am Geophys Union (EOS) 68:444

Knutson J, Green TH (1975) Experimental duplication of a high-pressure megacryst cumulate assemblage in a near-saturated hawaiite. Contrib Mineral Petrol 52:121–132

Langmuir CH (1986) Some possible geochemical consequences of in situ fractionation in a boundary layer. Am Geophys Union (EOS) 67:385

Langmuir CH (1988) Geochemical consequences of the solidification of magma chambers through "in situ" crystallization in a boundary layer. Nature (in press)

Lemarchand F, Villemant B, Calas G (1987) Trace element distribution coefficients in alkaline series. Geochim Cosmochim Acta 51:1071–1081

Maaloe S, Sorensen I, Hertogen J (1986) The trachybasaltic suit of Jan Mayen. J Petrol 27:439–466

Macdonald GA (1968) Composition and origin of Hawaiian lavas. Geol Soc Am Mem 116:477–522

Macdonald GA, Abbott AT, Peterson FL (1983) Volcanoes in the sea. University of Hawaii Press, Honolulu, 517 pp

Macdonald GA, Katsura T (1964) Chemical compositions of Hawaiian lavas. J Petrol 5:82–133

Mahood GA, Baker DR (1986) Experimental constraints on depths of fractionation of mildly alkalic basalts and associated felsic rocks: Pantelleria, Strait of Sicily. Contrib Mineral Petrol 93:251–264

McCallum IS, Charette MP (1978) Zr and Nb partition coefficients: implications for the genesis of mare basalts, KREEP, and sea floor basalts. Geochim Cosmochim Acta 42:859–869

Moore RB, Clague DA, Rubin M, Bohrson WA (1987) Hualalai Volcano: A preliminary summary of geologic, petrologic, and geophysical data: USGS Prof Paper 1350:571–585

Murck BW, Burress RC, Hollister LS (1978) Phase equilibria in fluid inclusions in ultramafic xenoliths. Am Mineral 63:40–46

Nash WP, Crecraft HR (1985) Partition coefficients for trace elements in silicic magmas. Geochim Cosmochim Acta 49:2309–2322

O'Hara MJ, Mathews RE (1981) Geochemical evolution in an advancing, periodically replenished, periodically tapped, continuously fractionated magma chamber. J Geol Soc London 138:237–277

Pearce JA, Norry MJ (1979) Petrogenetic implications of Ti, Zr, Y, and Nb variations in volcanic rocks. Contrib Mineral Petrol 69:33–47

Philpotts JA, Schnetzler CC (1970) Phenocryst-matric partition coefficients for K, Rb, Sr and Ba, with applications to anorthosite and basalt genesis. Geochim Cosmochim Acta 34:307–322

Porter SC (1972) Buried caldera of Mauna Kea Volcano, Hawaii. Science 175:1458–1460

Porter SC (1979) Quaternary stratigraphy and chronology of Mauna Kea, Hawaii. GSA Bull 90:980–1093

Rhodes JM (1983) Homogeneity of lava flows: Chemical data for historic Mauna Loa eruptions: J Geophys Res 88:869–879

Rhodes JM (1987) How Mauna Loa works: A geochemical perspective. In Abstr vol, Hawaii Symp on How Volcanoes Work. Hilo, Hawaii, p 208

Richard P, Shimizu N, Allegre CJ (1976) $^{143}Nd/^{144}Nd$, A natural tracer: An application to oceanic basalts. Earth Planet Sci Lett 31:269–278

Roedder E (1965) Liquid CO_2 inclusions in olivine-bearing nodules and phenocrysts from basalts. Am Mineral 50:1746–1782

Roedder E (1976) Petrologic data from experimental studies on crystallized silicate melt and other inclusions in lunar and Hawaiian olivine. Am Mineral 61:684–690

Roeder PL, Emslie RF (1970) Olivine-liquid equilibrium. Contrib Mineral Petrol 29:275–289

Sack RO, Walker D, Carmichael ISE (1987) Experimental petrology of alkalic lavas: constraints on cotectics of multiple saturation in natural basic liquids. Contrib Mineral Petrol 96:1–23

Shervais JW (1982) Ti-V plots and the petrogenesis of modern and ophiolitic lavas. Earth Planet Sci Lett 59:101–118

Spengler S, Garcia MO (1988) Geochemistry of Hawi lavas, Kohala Volcano, Hawaii. Contrib Mineral Petrol 99:90–104

Stearns HT, Macdonald GA (1946) Geology and ground-water resources of the island of Hawaii. Hawaii Div Hydrogr Bull 9:363

Suen CS, Frey FA (1987) Origins of the mafic and ultramafic rocks in the Ronda peridotite. Earth Planet Sci Lett 85:183–202

Sun SS (1980) Lead isotope study of young volcanic rocks from mid-ocean ridges, ocean islands and island arcs. Phil Trans R Soc London A-297:409–445

Thompson RN (1974) Primary basalts and magma genesis. I. Skye, North-West Scotland. Contrib Mineral Petrol 45:317–341

Todt W, Cliff RA, Hanser A, Hofmann AW (1984) $^{202}Pb + ^{205}Pb$ double spike for lead isotopic analyses. Terra Cognita 4:209

Watson EB, Green TH (1981) Apatite/liquid partition coefficients for the rare earth elements and strontium. Earth Planet Sci Lett 56:405–421

Wise WS (1982) A volume-time framework for the evolution of Mauna Kea Volcano, Hawaii. Am Geophys Union (EOS) 62:1137

Wise WS (1987) Evolution of Mauna Kea Volcano, Hawaii. In Abstr Vol, Hawaii Symp on How Volcanoes, Hilo, Hawaii, p 270

Wright TL, Fiske RS (1971) Origin of the differentiated and hybrid lavas of Kilauea Volcano, Hawaii. J Petrol 12:1–65

Wolfe EW (1987) Mauna Kea Summit and South Flank Fieldtrip Guidebook. GSA Cordilleran Section Meeting Guidebook, 38 pp

Wood DA (1979) A variably veined suboceanic uppermantle – genetic significance for mid-ocean ridge basalts from geochemical evidence. Geology 7:499–503